Received 14 July 2021; revised 17 August 2021; accepted 19 August 2021. Date of publication 10 September 2021; date of current version 27 September 2021.

Digital Object Identifier 10.1109/OJAP.2021.3111700

A Fully Transparent Wideband Water Patch Antenna With L-Shaped Feed

JIE SUN (Member, IEEE), AND KWAI-MAN LUK (Fellow, IEEE)

State Key Laboratory of Terahertz and Millimeter Waves, Department of Electrical Engineering, City University of Hong Kong, Hong Kong, SAR, China

CORRESPONDING AUTHOR: J. SUN (e-mail: sunjie1106@gmail.com)

This work was supported in part by the Research Grants Council of the Hong Kong, SAR, China, under Grant 9042990 (CityU 11215420), and in part by the Guangdong Provincial Department of Science and Technology, China, under Project 2020B1212030002.

ABSTRACT A wideband and fully optically-transparent water patch antenna is proposed. Both the patch and the ground plane are made of distilled water. Different from the previous water patch antennas, this proposed design features the utilization of an L-shaped distilled water probe as the feed structure. Thus, substantial improvement in the transparency is achieved. To excite the water patch antenna, a short inner probe of a coaxial cable is inserted into the water probe. The electromagnetic (EM) waves excited by the inner probe can propagate along the L-shaped water probe and also resonant in the middle substrate (air) under the water patch, causing radiation into the free space. The L-shaped water probe can significantly improve the impedance bandwidth, which has the same function as the reported L-shaped metallic probe. The results show that the proposed water patch antenna has a wide impedance bandwidth of 42.6% (from 1.48 to 2.28 GHz with $|S_{11}| < -10$ dB), a gain up to 7.5 dBi, a radiation efficiency up to 67% and broadside radiation pattern across the bandwidth. In addition, some parametric studies on the distilled water probe have been carried out for the design purpose. The proposed water patch antenna has confirmed the possibility of designing a patch antenna fully made of liquid or solid dielectric materials with high dielectric constant such as water, instead of using metal.

INDEX TERMS Optically-transparent antenna, water patch antenna, L-shaped water probe, wideband antenna.

I. INTRODUCTION

ANTENNAS composed of various liquids has drawn increasing attention in addition to the conventional metallic antennas [1]. These liquids include ionic liquid [2]–[3], ethyl acetate solution [4]–[5], pure water [6], etc. Among these liquids, water shows unique characteristics and advantages such as low material cost, easy accessibility, eco-friendly, large dielectric constant, highly optical transparency, etc. During past years, water had already been utilized to design various antennas, including dielectric resonator antenna [7]–[9], monopole [10]–[12], helix [13], spiral antenna [14], etc. Furthermore, water has also been used to adjust the performance characteristics of metallic antennas through functioning as a reflector [15]. These antenna designs enable water with more practical applications for the future communications.

Using pure water to design a patch antenna was proposed in 2015 [16]. Such design came from the concept of the dense dielectric patch antenna (DDPA), proposed in 2013 [17]. The DDPA simply utilizes a thin dielectric substrate with high dielectric constant to replace the top metallic patch while the remaining structures are kept the same as the conventional patch antenna. The results prove the DDPA can achieve almost the similar radiation performance as the metallic patch antenna, demonstrating the feasibility of simply using a substrate layer with a high dielectric constant to design a patch type antenna. Basically, pure water or distilled water utilized in the patch antenna can be considered as a pure liquid dielectric substrate with very high dielectric constant of around 80 at microwave frequencies [18]. Following this concept, a series of water patch antennas with both the patch and the ground plane composed of distilled water had been subsequently developed [18]–[21]. These designs have successfully achieve diverse radiation characteristics, including a monopole radiation pattern [18]–[19], the linear polarization [20] and the circular polarization [21]. However,

all these water patch antennas still require an indispensable metallic portion to excite the antenna. Thus, their entire structures actually are not fully made of water or liquid, even the feed structure is quite small in size.

In this paper, a fully water patch antenna is proposed. Substantial improvement in the transparency of the water patch antenna is achieved as the larger metallic L-shaped probe feed is replaced by the transparent water L-probe. Similar to the metallic L-probe used in [22]–[23], the size of the L-shaped water probe in this structure can also obviously affect the impedance bandwidth, but without influencing the radiation pattern too much. In order to obtain a wide bandwidth, the dimensions of the water probe need to be properly selected. The results demonstrate that this water patch antenna can achieve a wide impedance bandwidth of more than 40%, a gain up to 7.5 dBi, and a maximum radiation efficiency of 67% over the operating frequencies. The invention of this full-water patch antenna has successfully demonstrated the approach to designing patch antennas fully by the water or any dielectric substrates with a high dielectric constant instead of using metal.

This article is organized as follows. Section II introduces the antenna geometry. Section III illustrates the working principle of the antenna. Section IV displays the antenna performances and some relevant discussions. Finally, a conclusion is given in Section V.

II. ANTENNA GEOMETRY

The configuration and detailed dimensions of the proposed water patch antenna are shown in Fig. 1. The photos of the fabricated prototype are shown in Fig. 2. The patch, the ground plane and the L-shaped cylindrical probe are all composed of distilled water. The dielectric constant and dielectric loss tangent of distilled water used in this design can be found in [20]. Two vertical water walls are employed at the two edges of the ground plane in the H-plane (YOZ plane). The two vertical water walls can suppress the cross-polarization level in the H-plane at high frequencies [24]. The cross polarization level is relevant to the height of the water wall. Usually, a higher water wall can result in a smaller cross polarization level. In order not to increase the antenna profile, the height of the vertical water wall is selected to be the same as the height of water patch. All the distilled water are enclosed by the container made of transparent plexiglass. The dielectric constant and dielectric loss tangent of the plexiglass is 3.4 and 0.001 in the simulation. Some holes are left on the surface of the plexiglass container so that water can be injected into or drawn out by the injection syringe through the hole. After finishing injecting water into the container, the holes can be covered by the waterproof tape for the test. The middle substrate between the water patch and the water ground plane is air. For successfully feeding the antenna, a coaxial cable of 50 ohm was employed to connect the water patch and the testing equipment. The entire coaxial cable is designed to pass through the water ground plane into the middle substrate of air, with the purpose to

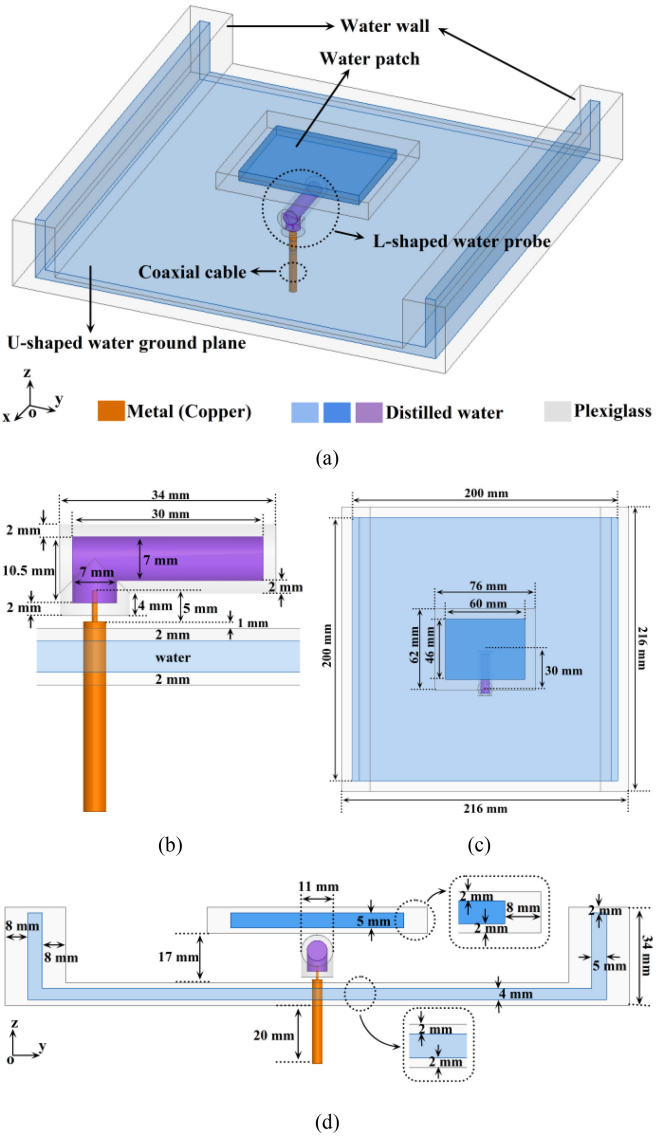

FIGURE 1. Geometry and dimension of the proposed water patch antenna fed by L-shaped water probe. (a) Perspective view, (b) Side view of the L-shaped water probe, (c) Top view, (d) Side view of the whole antenna.

transmit all the EM waves inside the coaxial cable into the middle substrate (air). However, if the antenna is fed only by the inner probe of a coaxial cable without a metallic L-shaped probe, the impedance matching is quite worse, which will be discussed in Section IV. Here, an L-shaped distilled water probe is employed as the feed. A short inner conductor of the coaxial cable was inserted into the water probe and the EM waves propagating along the surface of the water probe will excite the water patch antenna. The input impedance can also be different under different sizes of the water probe. More detailed studies on the water probe are given in Section IV.

III. WORKING PRINCIPLE

The current flowing on the conventional metallic L-shaped probe can feed the water patch by exciting the EM waves

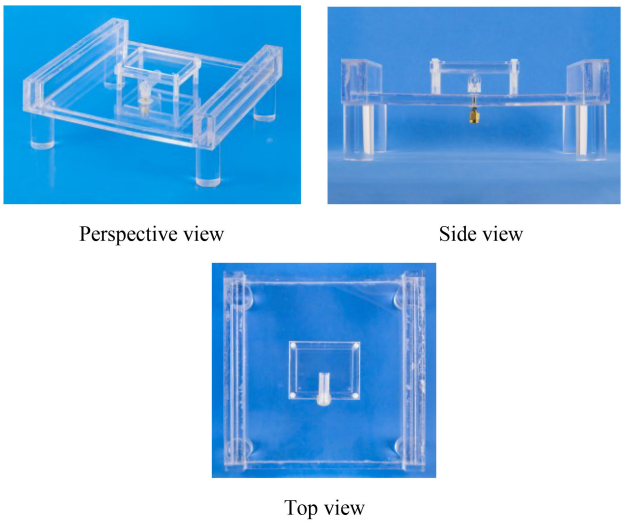

FIGURE 2. Photos of the fabricated full water patch antenna.

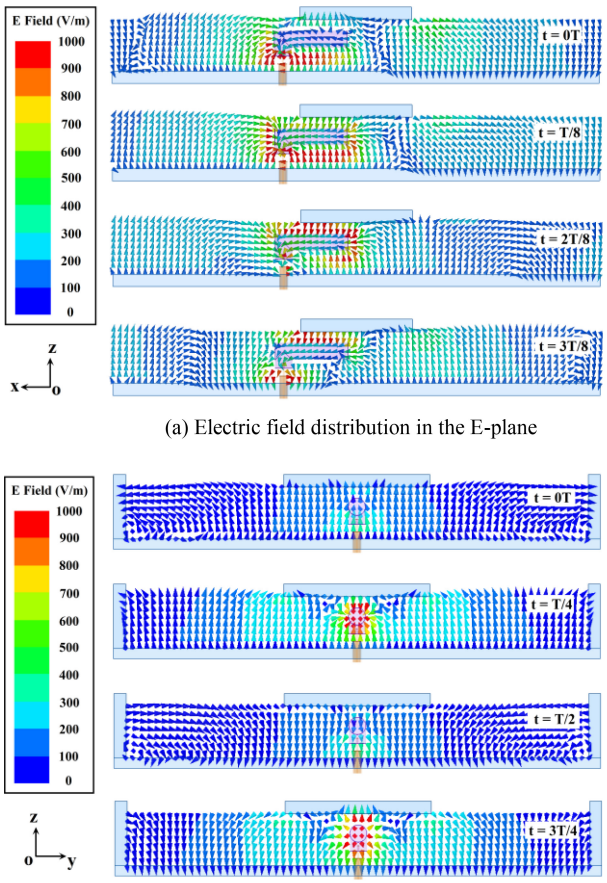

FIGURE 3. Electric field distribution at 1.8 GHz.

in the middle substrate under the patch. In this design, the L-shaped probe is completely composed of distilled water instead of metal. A short metallic probe is employed to insert the water probe. The metallic probe can excite the EM waves concentrated on the surface of the water

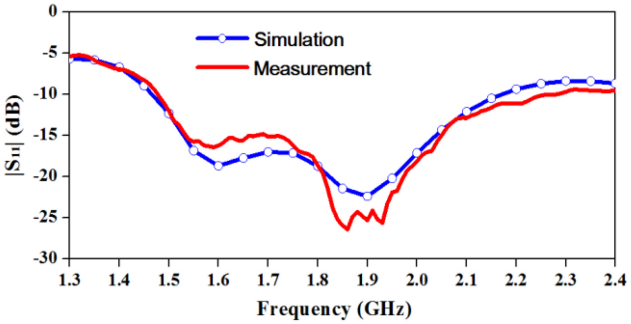

FIGURE 4. Simulated and measured $|S_{11}|$ of the proposed water patch antenna.

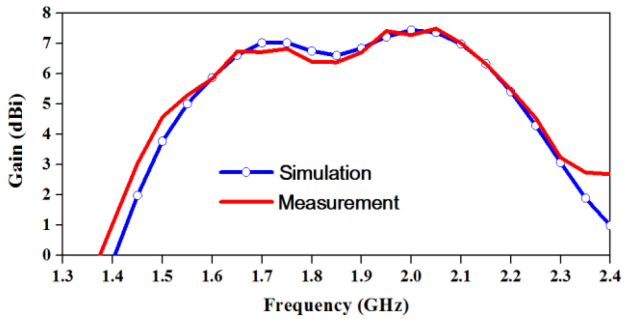

FIGURE 5. Simulated and measured gain of the proposed water patch antenna.

probe. These EM waves will be guided by the water probe, and propagate along the water probe from one end to the other end. Meanwhile, the movement of the EM waves on the surface of water probe can excite electric field (E-field) in the middle substrate, generating radiation characteristics then.

The distributions of the electric field in the middle substrate at 1.8 GHz are shown in Fig. 3. Fig. 3(a) shows that at the time t = 0T and t = T/8, where T refers to one period of time, the E-fields in the E-plane have a very strong magnitude among the bottom area of the water probe, and the E-fields have an opposite direction under the edge of the water patch. When at the time t = 2T/8 and t = 3T/8, the E-fields have a very strong magnitude among the top area of the water probe, and the direction of E-fields under the water patch are completely reversed when time t is 3T/8. The opposite E-fields under the two edges of the water patch form the linearly-polarized broadside radiation in the E-plane. The E-fields in the H-plane are shown in Fig. 3(b). At any moment over one period of time, the E-fields are almost uniform in magnitude except for the small area near water probe, and the E-field direction is the same under the two edges of the water patch. This ensures that the linearly-polarized broadside radiation in the H-plane will be cancelled out. The E-fields in the middle substrate are perpendicular to the surface of water, showing that the distilled water actually provides almost the same boundary effect as metal. These E-fields will resonant at certain frequencies under the water patch, and form radiation from the edges of the water patch to the free space.

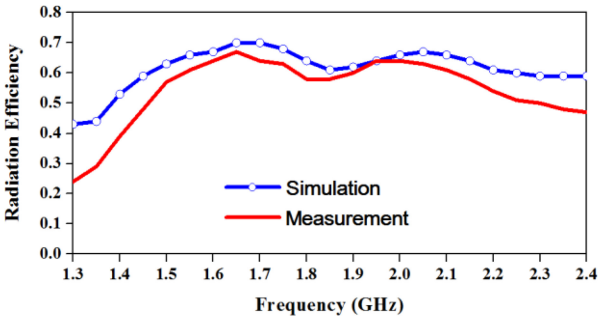

FIGURE 6. Simulated and measured radiation efficiency of the proposed water patch antenna.

IV. PERFORMANCE AND DISCUSSION

The antenna was fabricated and tested. The S-parameter was measured by Keysight ENA Network Analyzer E5080A. The gain, radiation pattern and efficiency were measured by Satimo StarLab Antenna Measurement System.

A. PERFORMANCE

The simulated and measured $|S_{11}|$ are shown in Fig. 4. The simulated bandwidth is 38.5% (from 1.47 to 2.17 GHz) while the measured bandwidth is 42.6% (from 1.48 to 2.28 GHz), both with $|S_{11}| < -10$ dB. Two minimum points appear at around 1.6 GHz and 1.9 GHz. The first minimum point is generated by the patch mode while the second minimum point is due to the L-shaped water probe. The two minimum points together form a wide impedance bandwidth of over 40%.

The simulated and measured gains are shown in Fig. 5. Good agreement has been achieved between simulation and measurement. The simulated gain changes from 2.5 dBi to 7.45 dBi, while the measured gain changes from 3 dBi to 7.5 dBi. The gain is small at lower frequencies, and increases up to 5.85 dBi at 1.6 GHz. Over the frequency range from 1.6 GHz to 2.15 GHz, both the simulated and measured gains are above 6.0 dBi. The result is similar to that of the metallic patch antenna.

The radiation efficiencies are shown in Fig. 6. The simulated radiation efficiency ranges from 60% to 70% while the measured one is between 50% and 67%, over their respective impedance bandwidth. The measured efficiency is lower than the simulated result.

The radiation patterns over the operating frequencies are shown in Fig. 7. Good agreement between the simulation and measurement can be observed. In the E-plane, the beam shifts into theta = 8 degree, which is caused by the existence of the water probe, leading to the asymmetry of the E-fields along the two aperture under the edges of the water patch. The cross-polarization level in the E-plane is below −20 dB and the back radiation level is about up to −10 dB. This is because some EM waves will penetrate through the water ground plane into the backward space. The radiation pattern in the H-plane is the broadside radiation, with the backlobe level of about −20 dB and the cross-polarization level of

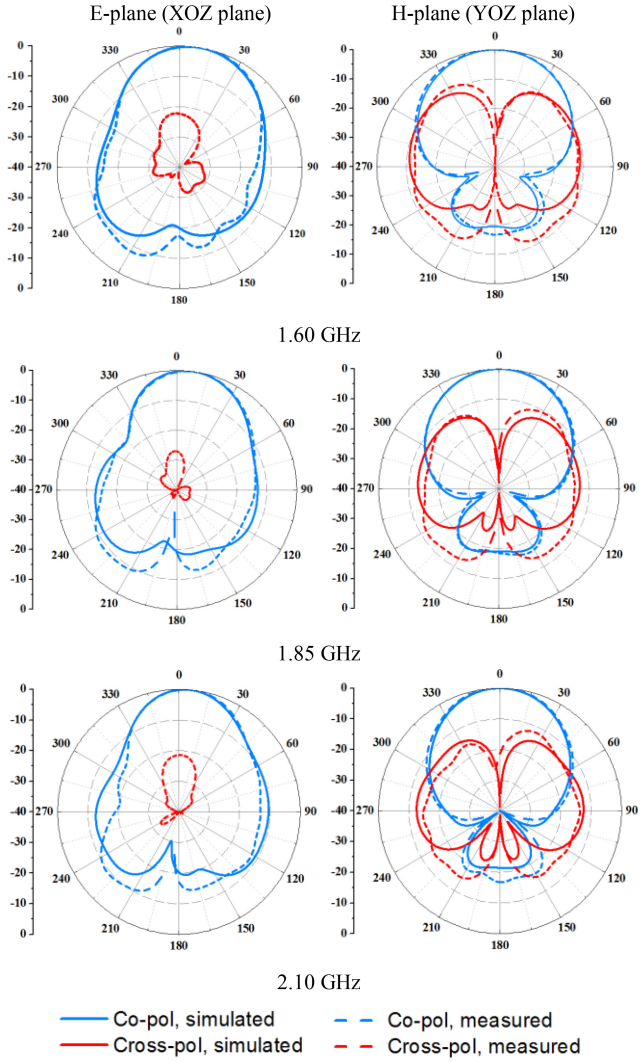

FIGURE 7. Simulated and measured radiation patterns over the operating band.

around −12 dB. The radiation from the water probe results in a higher cross-polarization level in the H-plane than that in the E-plane. By using two vertical water walls in the H-plane, the cross-polarization level at high frequencies is suppressed. Based on the studies in [24], higher vertical water walls can reduce more cross-polarization level in the H-plane. In this design, for not increasing the height of the whole antenna, the vertical water wall is in the same height of the water patch.

B. COMPARISON

A comparison of three types of patch antenna fed by L-shaped probe with broadside radiation pattern is given in Table 1. All of them operate at microwave frequencies with their patches and ground planes made either of metal or distilled water. It shows that the L-shaped feed probe, either composed of metal or water, can lead to a wide impedance bandwidth for a patch antenna with a thick substrate. The gains of water patch antenna fed by metallic or water probe are similar with less than 1.0 dB variation between each other. Two sidewalls made of water are employed in this

TABLE 1. Comparison of patch antennas with broadside radiation pattern fed by L-shaped probe.

Ref.	f_0 (GHz)	Material of patch	Material of ground plane	Material of L-shaped probe	Middle substrate	Imp. BW	Peak gain	Peak radiation efficiency
[20]	1.95	Distilled water	Distilled water	Copper	Air	34.9%	6.6 dBi	75%
[22]	4.53	Copper	Copper	Copper	Air	36%	~7.5dBi	N.A.
This work	**1.88**	**Distilled water**	**Distilled water**	**Distilled water**	**Air**	**43%**	**7.5 dBi**	**67%**

Imp. BW refers to the measured impedance bandwidth with $|S_{11}| < -10$ dB or SWR < 2.
N.A. refers to not available in the paper.

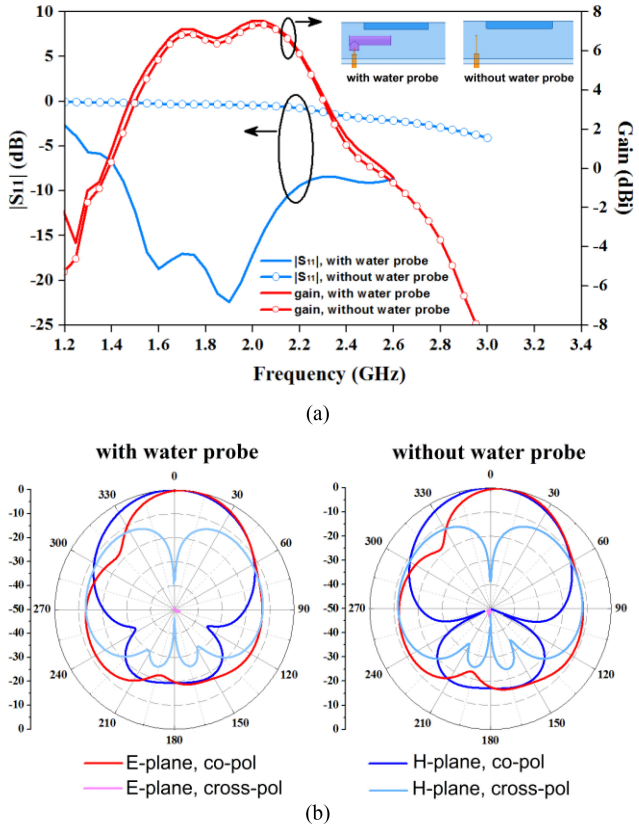

FIGURE 8. Simulated results: (a) $|S_{11}|$ and gain, (b) Radiation pattern at 1.8 GHz.

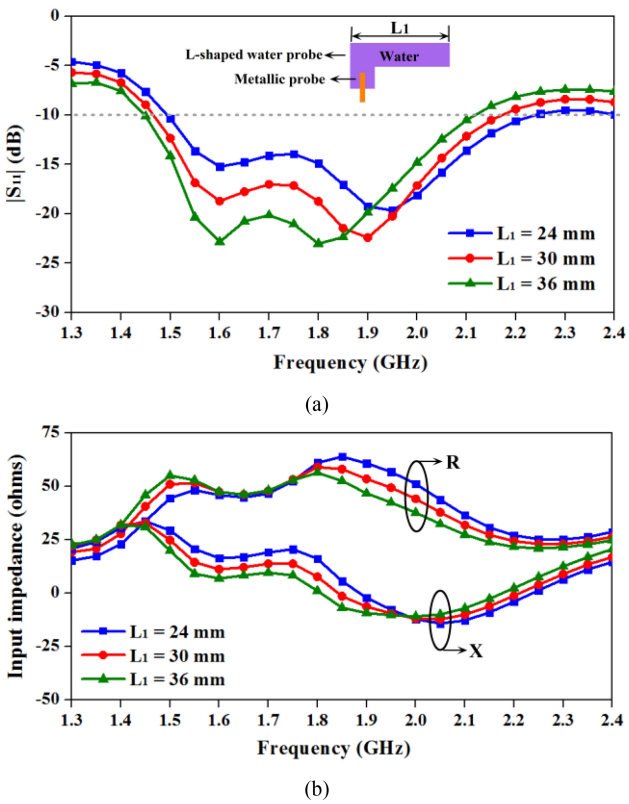

FIGURE 9. (a) Simulated $|S_{11}|$ versus frequency for different L_1; (b) Simulated input impedance versus frequency for different L_1.

work. The two sidewalls can concentrate radiation more in the broadside direction, thus, the peak gain in this work is higher than the result in [20]. The radiation efficiency of this proposed work is lower than the result in [20]. This is reasonable as the L-shaped water probe will dissipate certain E-field energy due to its dielectric loss. Although the efficiency in [22] is not available, considering it is all-metal structure, its radiation efficiency is very high.

C. DISCUSSION ON THE L-SHAPED WATER PROBE

The results of the proposed water patch antenna with and without L-shaped water probe are shown in Fig. 8. It turns out that when the proposed antenna is fed only by a vertical metal probe without the L-shaped water probe, the antenna can also achieve almost the same gain (not include the matching loss) and radiation pattern as that fed by an L-shaped water probe, demonstrating that the radiation is from the water patch rather than from the water probe. The length of vertical probe is adjusted to 15 mm in the middle substrate (air) in order to obtain a high gain. As shown obviously in Fig. 8(a), the use of L-shaped water probe can effectively improve the impedance bandwidth. Thus, the variation of the $|S_{11}|$ and input impedance with different dimensions of the L-shaped water probe are investigated, and the results are given in Figs. 9–12.

Fig. 9 shows the $|S_{11}|$ and input impedance for different horizontal length of water probe (L_1). When L_1 increases from 24 mm to 36 mm, the bandwidth shifts into lower frequency. A larger L_1 will increase the resistance at lower frequencies and reduce the input reactance at lower and middle frequencies.

Fig. 10 shows the $|S_{11}|$ and input impedance for different vertical length of water probe (L_2). Both the $|S_{11}|$ and input impedance are quite sensitive to the change of L_2. When L_2 increases from 9.5 mm to 11 mm, the impedance matching becomes better for the entire bandwidth with more $|S_{11}|$

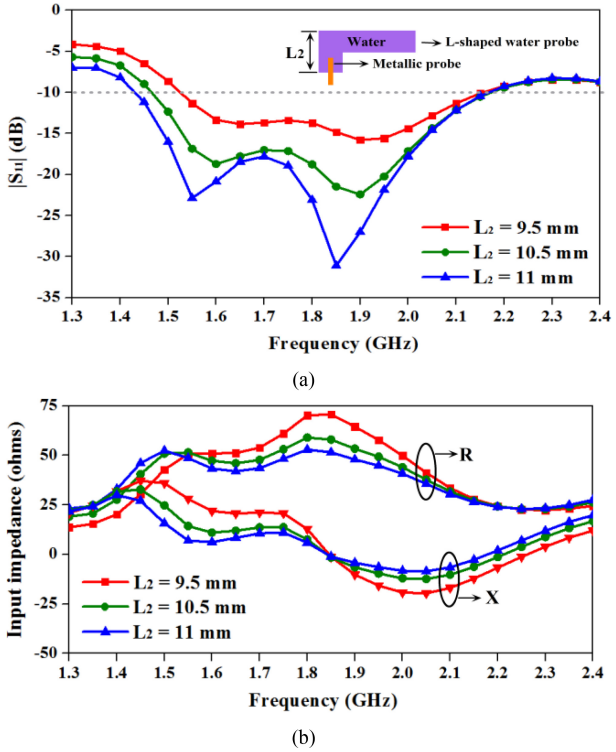

FIGURE 10. (a) Simulated $|S_{11}|$ versus frequency for different L_2; (b) Simulated input impedance versus frequency for different L_2.

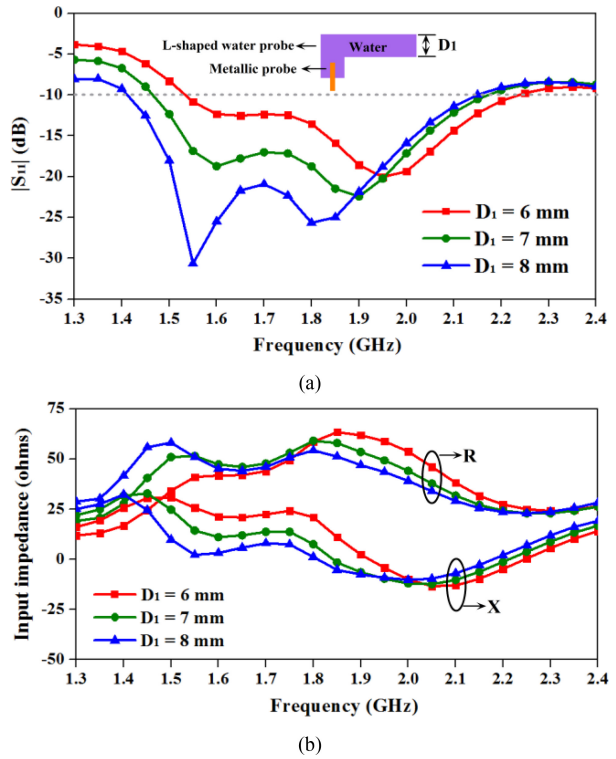

FIGURE 11. (a) Simulated $|S_{11}|$ versus frequency for different D_1; (b) Simulated input impedance versus frequency for different D_1.

having value below −15 dB. Based on the curves shown in Fig. 10(b), a larger L_2 can make the reactance closer to 0 ohm and the resistance closer to 50 ohm.

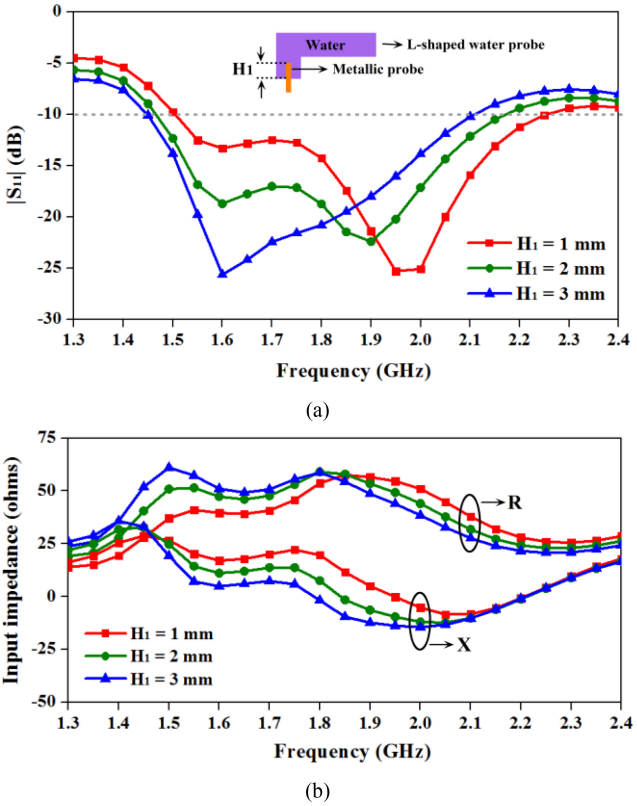

FIGURE 12. (a) Simulated $|S_{11}|$ versus frequency for different H_1; (b) Simulated input impedance versus frequency for different H_1.

Fig. 11 shows the $|S_{11}|$ and input impedance for different diameters of the water probe (D_1). When D_1 increases from 6 mm to 8 mm, the bandwidth entirely shifts into lower frequencies. Using a larger D_1 can improve the impedance matching at lower bands, as demonstrated in Fig. 11(b) that the resistance is close to 50 ohm and the reactance is close to 0 ohm.

Fig. 12 shows the $|S_{11}|$ and input impedance for different metal length that inserted into the water feed probe (H_1). When H_1 increases from 1 mm to 3 mm, the bandwidth shifts into lower frequencies. Among the low frequencies, the resistance is close to 50 ohm and the reactance is close to 0 ohm with a larger H_1.

D. DESIGN GUIDELINE

1) Choose a larger thickness for both the water patch and the water ground plane in case the practical value is smaller than the simulated one. It is recommended to choose a thickness slightly greater than or equal to 4 mm for this water patch antenna working at around 2 GHz.

2) A thicker middle substrate can be selected to achieve a wider impedance bandwidth.

3) Since the container (plexiglass) will also be part of the middle substrate, smaller thickness of the plexiglass is recommended as it will not affect the dielectric constant of the middle hybrid substrate too much.

4) The proposed water patch antenna mainly operates in the patch mode. However, considering that part of EM waves can resonant inside water and also radiate from water, the variation of the thickness for the water patch and the water ground plane will affect the bandwidth, as already illustrated in [20]. This also explains why the water patch antenna and the metallic patch antenna have different resonant frequencies even though they have the same patch size.

5) The employment of the L-shaped water probe can significantly improve the bandwidth. Based on the parametric studies in this paper, using a larger vertical length of the water probe (L_2) and a larger diameter of the water probe (D_1) are recommended to obtain a wide bandwidth.

V. CONCLUSION

In this paper, a wideband water patch antenna fed by an L-shaped water probe is proposed. Both the patch, the ground plane and the feed probe are composed of distilled water. By using the transparent plexiglass as the container to fix water, the total water patch antenna can obtain fully optical transparency. The L-shaped water probe, can not only excite EM waves in the middle substrate, but can also enhance the impedance bandwidth significantly. The variation of the water probe dimensions can cause obvious change on the antenna input impedance. The detailed parametric studies of the water probe were investigated with the results given in this paper. The proposed configuration in this paper demonstrates that a patch antenna can be designed entirely by dielectric materials with very high permittivity, such as water.

ACKNOWLEDGMENT

The authors would like to thank Chun Kwong LAU for his careful fabrication of this antenna.

REFERENCES

[1] Y. Huang, L. Xing, C. Song, S. Wang, and F. Elhouni, "Liquid antennas: Past, present and future," *IEEE Open J. Antennas Propag.*, vol. 2, pp. 473–487, 2021.

[2] C. Song, E. L. Bennett, J. Xiao, A. Alieldin, K.-M. Luk, and Y. Huang, "Metasurfaced, broadband, and circularly polarized liquid antennas using a simple structure," *IEEE Trans. Antennas Propag.*, vol. 67, no. 7, pp. 4907–4913, Jul. 2019.

[3] C. Song, E. L. Bennett, J. Xiao, Q. Hua, L. Xing, and Y. Huang, "Compact ultra-wideband monopole antennas using novel liquid loading materials," *IEEE Access*, vol. 7, pp. 49039–49047, 2019.

[4] J. Ren *et al.*, "Radiation pattern and polarization reconfigurable antenna using dielectric liquid," *IEEE Trans. Antennas Propag.*, vol. 68, no. 12, pp. 8174–8179, Dec. 2020..

[5] Z. Chen and H. Wong, "Liquid dielectric resonator antenna with circular polarization reconfigurability," *IEEE Trans. Antennas Propag.*, vol. 66, no. 1, pp. 444–449, Jan. 2018.

[6] C. Hua *et al.*, "Reconfigurable antennas based on pure water," *IEEE Open J. Antennas Propag.*, vol. 2, pp. 623–633, 2021.

[7] S. G. O'Keefe and S. P. Kingsley, "Tunability of liquid dielectric resonator antennas," *IEEE Antennas Wireless Propag. Lett.*, vol. 6, pp. 533–536, 2007.

[8] R. E. Jacobsen, A. V. Lavrinenko, and S. Arslanagić, "A water-based huygens dielectric resonator antenna," *IEEE Open J. Antennas Propag.*, vol. 1, pp. 493–499, 2020.

[9] L. Xing *et al.*, "A high-efficiency wideband frequency- reconfigurable water antenna with a liquid control system: Usage for VHF and UHF applications," *IEEE Antennas Propag. Mag.*, vol. 63, no. 1, pp. 61–70, Feb. 2021.

[10] L. Xing, Y. Huang, Y. Shen, S. Al Ja'afreh, Q. Xu, and R. Alrawashdeh, "Further investigation on water antennas," *IET Microw. Antennas Propag.*, vol. 9, no. 8, pp. 735–741, 2015.

[11] C. Hua, Z. Shen, and J. Lu, "High-efficiency sea-water monopole antenna for maritime wireless communications," *IEEE Trans. Antennas Propag.*, vol. 62, no. 12, pp. 5968–5973, Dec. 2014.

[12] C. Hua and Z. Shen, "Shunt-excited sea-water monopole antenna of high efficiency," *IEEE Trans. Antennas Propag.*, vol. 63, no. 11, pp. 5185–5190, Nov. 2015.

[13] Z. Ren, S. Qi, Z. Hu, Z. Shen, and W. Wu, "Wideband water helical antenna of circular polarization," *IEEE Trans. Antennas Propag.*, vol. 67, no. 11, pp. 6770–6777, Nov. 2019.

[14] Z. Hu, S. Wang, Z. Shen, and W. Wu, "Broadband polarization-reconfigurable water spiral antenna of low profile," *IEEE Antennas Wireless Propag. Lett.*, vol. 16, pp. 1377–1380, 2017.

[15] J.-J. Liang, G.-L. Huang, K.-W. Qian, S.-L. Zhang, and T. Yuan, "An azimuth-pattern reconfigurable antenna based on water grating reflector," *IEEE Access*, vol. 6, pp. 34804–34811, 2018.

[16] Y. Li and K.-M. Luk, "A water dense dielectric patch antenna," *IEEE Access*, vol. 3, pp. 274–280, 2015.

[17] H. W. Lai, K.-M. Luk, and K. W. Leung, "Dense dielectric patch antenna—A new kind of low-profile antenna element for wireless communications," *IEEE Trans. Antennas Propag.*, vol. 61, no. 8, pp. 4239–4245, Aug. 2013.

[18] J. Sun and K.-M. Luk, "A wideband low cost and optically transparent water patch antenna with omnidirectional conical beam radiation patterns," *IEEE Trans. Antennas Propag.*, vol. 65, no. 9, pp. 4478–4485, Sep. 2017.

[19] J. Sun and K.-M. Luk, "A compact-size wideband optically-transparent water patch antenna incorporating an annular water ring," *IEEE Access*, vol. 7, pp. 122964–122971, 2019.

[20] J. Sun and K.-M. Luk, "A wideband and optically transparent water patch antenna with broadside radiation pattern," *IEEE Antennas Wireless Propag. Lett.*, vol. 19, no. 2, pp. 341–345, Feb. 2020.

[21] J. Sun and K.-M. Luk, "A circularly polarized water patch antenna," *IEEE Antennas Wireless Propag. Lett.*, vol. 19, no. 6, pp. 926–929, Jun. 2020.

[22] C. L. Mak, K. M. Luk, K. F. Lee, and Y. L. Chow, "Experimental study of a microstrip patch antenna with an L-shaped probe," *IEEE Trans. Antennas Propag.*, vol. 48, no. 5, pp. 777–783, May 2000.

[23] Y.-X. Guo, C.-L. Mak, K.-M. Luk, and K.-F. Lee, "Analysis and design of L-probe proximity fed-patch antennas," *IEEE Trans. Antennas Propag.*, vol. 49, no. 2, pp. 145–149, Feb. 2001.

[24] Y.-X. Guo, K.-M. Luk, and K.-F. Lee, "L-probe fed thick-substrate patch antenna mounted on a finite ground plane," *IEEE Trans. Antennas Propag.*, vol. 51, no. 8, pp. 1955–1963, Aug. 2003.

[25] K. F. Lee, K. M. Luk, and H. W. Lai, *Microstrip Patch Antennas*, 2nd ed. Hackenack, NJ, USA: World Sci., 2018.

JIE SUN (Member, IEEE) was born in Nanjing, China. He received the Ph.D. degree in electrical engineering from the City University of Hong Kong.

He is currently a Research Fellow with the State Key Laboratory of Terahertz and Millimeter Waves, Department of Electrical Engineering, City University of Hong Kong. His research interests include water patch antennas, liquid antennas, dense dielectric patch antennas, wideband millimeter-wave printed antennas, and arrays.

Dr. Sun was the recipient of Best Student Paper Award in the 2017 IEEE International Workshop on Electromagnetics: Applications and Student Innovation Competition (iWEM), held at University College London, U.K. He was also the winner (1st) of the Student Innovation Poster Competition in the iWEM 2019, Qingdao, China. He was the Secretary of the IEEE (HK) Section AP/MTT Joint Chapter in 2020. He was the Publication Co-Chair of the 2020 Asia–Pacific Microwave Conference and the 2021 Cross Strait Radio Science and Wireless Technology Conference.

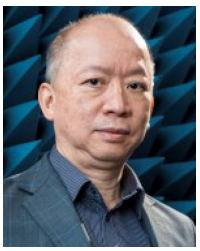

KWAI-MAN LUK (Fellow, IEEE) received the B.Sc. (Eng.) and Ph.D. degrees in electrical engineering from The University of Hong Kong in 1981 and 1985, respectively.

In 1985, he joined the Department of Electronic Engineering, City University of Hong Kong, as a Lecturer. Two years later, he moved to the Department of Electronic Engineering, The Chinese University of Hong Kong, where he spent four years. In 1992, he returned to the City University of Hong Kong, where he served as Head of the Department of Electronic Engineering from 2004 to 2010, and the Director of the State Key Laboratory of Millimeter Waves from 2008 to 2013, and is currently the Chair Professor of Electrical Engineering. He has authored four books, 11 research book chapters, over 398 journal papers and 280 conference papers. He was awarded 15 U.S. and more than 10 PRC patents on the design of a wideband patch antenna with an L-shaped probe feed. His recent research interests include design of patch antennas, magneto-electric dipole antennas, dense dielectric patch antennas and open resonator antennas for various wireless applications.

Dr. Luk received the Japan Microwave Prize, at the 1994 Asia–Pacific Microwave Conference held in Chiba in December 1994, the Best Paper Award at the 2008 International Symposium on Antennas and Propagation, Taipei, in October 2008, and the Best Paper Award at the 2015 Asia–Pacific Conference on Antennas and Croucher Foundation Senior Research Fellow in Hong Kong. He received the 2011 State Technological Invention Award (2nd Honor) of China. He is the recipient of the 2017 IEEE APS John Kraus Antenna Award. He received the prestigious 2019 Ho Leung Ho Lee Prize for Science and Technology Progress. He was Technical Program Chairperson of the 1997 Progress in Electromagnetics Research Symposium, the General Vice-Chairperson of the 1997 and 2008 Asia–Pacific Microwave Conference, the General Chairman of the 2006 IEEE Region Ten Conference, the Technical Program Co-Chairperson of 2008 International Symposium on Antennas and Propagation, and the General Co-Chairperson of 2011 IEEE International Workshop on Antenna Technology, the General Co-Chair of 2014 IEEE International Conference on Antenna Measurements and Applications, and the General Co-Chair of 2015 International Conference on Infrared, Millimeter, and Terahertz Waves in 2015. He was the General Chair of the 2020 Asia–Pacific Microwave Conference, Hong Kong. He was a Chief Guest Editor for a special issue on "Antennas in Wireless Communications" published in the PROCEEDINGS OF THE IEEE in July 2012. He is a Deputy Editor-in-Chief of *Progress in Electromagnetics Research* and an Associate Editor of *IET Microwaves, Antennas and Propagation*. He is a Member of the Editor Board for *Engineering* and the Chinese Academy of Engineering. He is a member of IEEE APS Administrative Committee Member from 2021 to 2023. He is a fellow of the Chinese Institute of Electronics, PRC, the Institution of Engineering and Technology, U.K., the Institute of Electrical and Electronics Engineers, USA, the Electromagnetics Academy, USA, and the U.K. Royal Academy of Engineering.